Dynamical density functional theory for glassy behaviour

2002 J. Phys.: Condens. Matter 14 12203

(http://iopscience.iop.org/0953-8984/14/46/322)

INSTITUTE OF PHYSICS PUBLISHING JOURNAL OF PHYSICS: CONDENSED MATTER

J. Phys.: Condens. Matter **14** (2002) 12203–12222 PII: S0953-8984(02)39065-9

Dynamical density functional theory for glassy behaviour

Kazuhiro Fuchizaki[1] **and Kyozi Kawasaki**[2]

[1] Department of Physics, Ehime University, Matsuyama 790-8577, Japan
[2] 4-37-9 Takamidai, Higashi-ku, Fukuoka 811-0215, Japan

E-mail: fuchizak@phys.sci.ehime-u.ac.jp

Received 3 July 2002
Published 8 November 2002
Online at stacks.iop.org/JPhysCM/14/12203

Abstract

Glassy dynamics of fluid particles in a supercooled liquid is discussed on the basis of the time-evolution equation obtained through the dynamical density functional theory (DDFT). The advantage, brought about by the coarse-grained nature of the formalism, in treating such strongly correlated motion over other approaches, such as the mode-coupling theories and direct computer simulations, is emphasized. A direction in which the DDFT should prove its worth on examining the phenomena is suggested.

1. Introduction

The classical density functional theories have matured to open up a new paradigm in investigating fundamental aspects of inhomogeneous fluid physics and related areas. Among the vast area of topics concerned, this paper will contribute to the problem of slow dynamics in supercooled liquids near their glass transition points.

The problem has been studied for more than a century not only by physicists but also by chemists and engineers without achieving any crucial understanding on the phenomena until the pioneering mode-coupling theories (MCT) appeared in the mid-1980s [1]. The solution of the mode-coupling equation addressed the glass transition as an ergodic-to-non-ergodic transition. The discovery of the fascinating consequences on the singularity and the scaling properties around the transition has led to a subsequent explosion in research in this field. The current understanding of the phenomena would never have been attained without MCT and this paper begins with a brief overview on the glassy dynamics from the viewpoint of MCT. Experimental as well as computer simulation research stimulated by MCT over more than a decade, however, have offered clear-cut evidence showing the limitation of MCT at the same time [2]. This was our initial motivation to devise and develop a new framework that should overcome the deficiencies of MCT. This point will be touched on in the latter half of this section before introducing our strategy, the dynamical density functional (DDF) formalism,

0953-8984/02/4612203+20$30.00

in the next section. Since the derivation of our DDF equation and the procedure with which to obtain numerical solutions to it have already been published elsewhere [3–7], they will be only outlined here, emphasizing the underlying philosophy of *coarse-graining*. The concept of coarse-graining or contraction of information should be the guiding principle along which to proceed and is stressed throughout the present paper. In the third section, our published results describing the general features of slow dynamics in a supercooled liquid will be first reviewed. This includes the result which has never been obtained through the original version of MCT. Then, the advantage brought about by the coarse-grained nature of the DDF formalism will be discussed. Some new results are presented. The last section is devoted to discussion, in which other DDF approaches will be referred to. Also we shall respond to the criticism raised by the latter. In order to render the paper useful to general readers further investigations are suggested which will deepen our understanding of the phenomena. A further comment is included in the appendix.

Although many kinds of liquids, which include polymer solutions, ionic and molecular liquids other than simple liquids, have been examined and even classified according to their manner of structural relaxation [8], we focus only on the hard-sphere system (HSS) in this paper. This is because not only can analytic calculations sometimes be performed for HSS but also HSS serves as the *reference system* for subsequent perturbation calculations of liquids with more realistic interactions [9]. The HSS is supposed to be experimentally realized by a suspension of identical colloidal spheres stabilized by thin macromolecular surface layers [10]. The latter has been extensively studied utilizing dynamic light scattering spectroscopy to accumulate results [11–14] which are to be compared with those put forth by theories. However, care must be taken when comparing the theoretical treatments for HSS with the experimental results obtained for a colloidal suspension, because the former, including ours, neglect the hydrodynamic interactions present in an actual colloidal suspension. Indeed, Tokuyama and Oppenheim [15] claimed, through the calculation of the transport coefficient obtained from a suitable spatio-temporal coarse-graining of the set of Langevin equations of motion of the colloidal particles interacting hydrodynamically as well as directly, that the hydrodynamic interactions can affect not only the short-time dynamics but also the long-time dynamics in which the structural relaxation occurs. Whether their results can reproduce the experimental results as well as MCT remains to be seen.

1.1. Brief overview of glassy dynamics in supercooled liquids

The MCT were originally designed to deal with the cage effect in dense liquids. To this end, the Zwanzig–Mori type [16] time-evolution equation for the normalized density correlator $\phi_q(t) \equiv S(q,t)/S(q)$ was set up first [1], where $S(q,t)$ and $S(q) = S(q,t=0)$ are the density autocorrelation functions or the so-called intermediate scattering function and the static structure factor, respectively. The former is given by $S(q,t) = \langle \delta\rho_{\boldsymbol{q}}(t)\delta\rho_{-\boldsymbol{q}}(0)\rangle/N$, where N is the total number of particles in the system and $\delta\rho_{\boldsymbol{q}}$ is the spatial Fourier transform of the local density fluctuation $\delta\rho(\boldsymbol{r}) \equiv \rho(\boldsymbol{r}) - \rho_0$, $\rho_0 = \langle\rho\rangle$ being the average density.

Then, in the original MCT, a mode-coupling approximation, in which the memory kernel was expressed as a quadratic function of $\phi_q(t)$, was invoked to obtain a closed set of coupled equations for $\phi_q(t)$. The resultant self-consistent equation exhibited a fold-type bifurcation for the time evolution of $\phi_q(t)$. That is, as supercooling proceeds beyond the equilibrium freezing point, there is a point beyond which ϕ_q never decays to zero but to some positive value f_q, called the glass form factor. Here, the control parameter governing the degree of supercooling, the packing fraction η for HSS, enters through $S(q)$, which is the input information to the mode-coupling equation. Thus, the original MCT addressed the liquid-to-glass transition

as the ergodic-to-non-ergodic transition. In this context f_q is also called the non-ergodicity parameter. It is noted that the singularity obtained through MCT is *not* associated with the dynamical variable with built-in critical divergence but is purely kinetic in origin.

The MCT have revealed in this way not only the novel feature of the liquid–glass transition, which is different from that of the conventional thermal phase transitions, but also the 'universal' character of the relaxation scenario near the transition point as follows [17]. The separation parameter $\epsilon \equiv (\eta - \eta_c)/\eta_c$, η_c being the critical packing fraction at which ergodicity breaks down, was introduced, which measures the distance from criticality. The original MCT predictions were then expressed as the asymptotic scaling forms that are correct only in leading order in ϵ. MCT thus predicted that beyond the microscopic timescale t_0 of the order of the reciprocal of phonon frequency the density correlator shows the first critical decay, called the β-relaxation, with the characteristic timescale $t_\epsilon = t_0|\epsilon|^{-1/(2a)} \gg t_0$, which diverges as η tends toward η_c with the exponent $1/(2a)$ $(0 < a < 1/2)$. In the β-relaxation regime the density correlator was shown to obey $\phi_q(t) = f_q^c + h(q)\sqrt{\epsilon}\, g_\pm(t/t_\epsilon)$, which implies that spatial and temporal dependencies are separated and is known as the *factorization property*. Neither the non-ergodicity parameter at criticality f_q^c, the critical amplitude $h(q)$ nor the 'universal' function $g_\pm$, called the β-correlator ($\pm$ corresponding to the sign of ϵ), depend on $|\epsilon|$, and hence on η. The β-correlator can be computed if the one parameter λ, called the exponent parameter which is in turn obtained from $S(q)$, is given. However, in the early β-relaxation regime, $g_\pm$ can be given by a power-law form $g_\pm(t) \sim t^{-a}$ $(t \ll 1)$. The exponent a is the same as that which appeared in the β-relaxation timescale t_ϵ.

The divergence of t_ϵ and the decay of the β-relaxation governed by the β-correlator toward $\epsilon \to 0_\pm$ is an aspect that expresses a liquid particle going to be arrested in a cage formed by the surrounding particles. However, a further relaxation is possible on the $\epsilon < 0$ side by cage breakdown and hence allowing large-scale diffusion. This process is called α-relaxation. The late β-relaxation regime continuously crosses over to the early α-relaxation regime so that the decay law may be obtained by the asymptotic expansion of g_-. Indeed, the original version of MCT yielded a different power law $g_-(t) \sim -t^b$ $(t \gg 1)$, which is also known as the von Schweidler law. The exponent b $(0 < b \leqslant 1)$ is related to a as well as to λ via $\Gamma(1-a)^2/\Gamma(1-2a) = \Gamma(1+b)^2/\Gamma(1+2b) = \lambda$. The manner of the α-relaxation is characterized by the so-called *time–temperature superposition principle*, which is also valid to leading order in ϵ, implying that the time variations of the density correlator for various ϵ (<0) fall on a single curve when the time is suitably scaled; $\phi_q(t) = \Phi(t/\tau)$. The original MCT showed that the α-relaxation timescale diverges as $\epsilon \to 0_-$ with the power law $\tau \sim D^{-1} \sim |\epsilon|^{-\gamma}$, where D is the self-diffusion coefficient. The exponent γ is related to the exponents a and b by $\gamma = 1/(2a) + 1/(2b)$. The master function Φ, though not universal in that the functional form depends on the probing quantity, is well described by the stretched exponential function $\phi_q(t) \sim \exp[-(t/\tau_q)^{\beta_q}]$. However, this is shown to be correct only in the limit $q \to \infty$, where β_q tends to b of the von Schweidler law [18].

These predictions were extensively tested by various laboratory experiments and computer simulations, and were thoroughly reviewed [19, 20]. Those results that concern HSS are summarized in table 1. As seen from table 1 the agreement between the MCT predictions and experimental results is quite satisfactory. This is because the colloid particles are so large in size that the effect of thermal fluctuations is quite ineffective, as far as hydrodynamic forces mediated by a solvent are considered to be negligible at long times, and complete structural arrest is attained within the timescale of experimental observations. The effects of thermal fluctuations, not taken into consideration in the original MCT, are the very effects that trigger restoration of ergodicity in other glass forming systems.

Table 1. The result of experimental tests regarding the scaling properties of density correlators measured by dynamic light scattering spectroscopy for colloidal hard spheres. a and γ are the exponents that specify the β- and α-relaxation timescales, respectively, whereas b is obtained through the asymptotic expansion of the β-correlator (see text).

	MCT predictions [21]	Experimental tests
Critical packing fraction	$\eta_c = 0.525$	$0.574 < \eta_c < 0.581$ $\eta_f = 0.494$[a] $\eta_m = 0.543$[b]
Scaling regime	Scaling properties	
β-relaxation	Factorization property	Demonstrated in figure 4 of [11] ($\epsilon \lessgtr 0$) figure 8 of [12] ($\epsilon > 0$) figure 14 of [13] ($\epsilon \lessgtr 0$)
	Glass form factor and critical amplitude	Demonstrated in figure 2 of [11] ($\epsilon \lessgtr 0$) figure 7 of [12] ($\epsilon > 0$) figure 10 of [13] ($\epsilon \lessgtr 0$)
	Exponents $a = 0.301$ $b = 0.545$	Compared in figure 3 of [11] figure 11 of [13]
α-relaxation	Time–temperature superposition principle	Demonstrated in figure 4 of [11] figure 13 of [13]
	$\gamma = 2.58$	Compared indirectly in figure 3 of [11] figure 11 of [13]

[a] Freezing point.
[b] Melting point.

1.2. Need for a coarse-grained description

The original version of MCT described above captured the cage effect by the nonlinear coupling between ϕ_q's entering in the memory kernel, which becomes stronger with increasing density fluctuation toward the ergodic-to-non-ergodic transition point until the structure is completely frozen in. However, in real materials, this transition is avoided due to a residual activation process, called the hopping process, caused by thermal fluctuations. In order to take this effect into account, the original MCT were patched up in such a way that the nonlinear coupling to currents $\dot{\phi}_q$ is included. The new version is often referred to as the extended MCT [22, 23], which is characterized, in short, by an inclusion of the temperature (packing fraction)-dependent hopping parameter δ. In the simplest case in which $S(q)$ is given by a single δ peak, the time variation of the density correlator was numerically solved to show that the system always remains ergodic [22]. However, the determination of δ in the usual cases is too involved so that δ is merely taken as a fitting parameter with which to adjust the β-correlator [24].

With this circumstance in mind, the dynamical density functional theory (DDFT) was designed [3] to naturally involve the effect of thermal fluctuations. The MCT treatments for the glassy dynamics around the singularity remind us of those for the critical dynamics, although the singularities in the latter are caused by underlying critical point singularity. Then, in view of the fact that the shortcoming of the original MCT arises from their mean-field character,

the effects of thermal fluctuations would be incorporated most naturally by constructing an appropriate mesoscopic kinetic equation based on the analogy of the strategy taken in the theoretical development of the critical dynamics [25]. That is, what we need is to set up a set of time-evolution equations involving only spatio-temporally slowly varying variables, the so-called gross variables in the critical dynamics nomenclature, which are coarse-grained up to the spatio-temporal scales of the problem in question.

One of the trials in this direction was the nonlinear fluctuating hydrodynamics developed by Das and Mazenko [26], in which the local velocity field as well as the local density was chosen as the gross variable. However, physical insight is required for the choice of gross variables because, unlike in the critical dynamics, no general prescription is available. In our DDFT, only the density has been retained based on a heuristic argument of Cohen and de Schepper [27], substantiated later [28], that the local momentum and energy densities may quickly be transferred among the particles especially in a dense fluid but the particles themselves are not easy to rearrange.

The coarse-grained description will, at the same time, bring about an effective access to the slow relaxation regime through the renormalization of the microscopic dynamical effects to the appropriate transport coefficients. This is evident as seen from the time-dependent Ginzburg–Landau treatment of, for example, the phase ordering kinetics [29]. One of our purposes in this review is to introduce some useful aspects of DDFT.

In summary, by introducing a coarse-grained kinetic equation for the density, we are aiming at capturing the essential part of the long-time behaviour of the glassy dynamics. It should be mentioned that what was done in the original MCT is an extraction of temporally slowly varying components of the density correlator with the characteristic timescales of the β- and α-relaxations from the mode-coupling equation derived on the microscopic basis. The DDFT takes over the spirit of coarse-graining and is believed to be justifiable in this context.

2. Dynamical density functional theory

2.1. Formulation

Microscopically time evolution of the state specified by a set of microscopic variables $\{a\}$ is described by the time-evolution equation for the distribution function $\mathcal{P}(\{a\}, t)$, which is in general given by

$$\partial_t \mathcal{P}(\{a\}, t) = \mathcal{L}\{a\}\mathcal{P}(\{a\}, t), \tag{1}$$

where $\mathcal{L}$ stands for a Liouville operator defined in the space $\{a\}$. For a colloidal system consisting of N colloid spheres, a suitable choice for this microscopic description is the Smoluchowski equation in which $\{a\}$ is taken as $\{\boldsymbol{R}_i\} \equiv \boldsymbol{R}^N$, where $\boldsymbol{R}_i$ $(i = 1, \ldots, N)$ is the position vector of the ith particle. $\mathcal{P}$ in (1) now represents the N-body distribution function $P_N(\boldsymbol{R}^N, t)$ and the equation is [30]

$$\partial_t P_N(\boldsymbol{R}^N, t) = \Omega_N(\boldsymbol{R}^N) P_N(\boldsymbol{R}^N, t), \tag{2}$$

where $\Omega_N(\boldsymbol{R}^N) = D_0 \nabla^N \cdot [\nabla^N + \beta \nabla^N U_N(\boldsymbol{R}^N)]$, D_0 is the Stokes–Einstein diffusion coefficient, $\beta = 1/(k_\mathrm{B}T)$ (the reciprocal of the temperature divided by the Boltzmann constant k_B) and $U_N(\boldsymbol{R}^N)$ is the total potential energy.

We now coarse-grain (2). To this end we divide the whole system into an assembly of cells of volume v_c, each labelled by a vector $\boldsymbol{n}$ with integer components. This cell is macroscopically small but microscopically still large enough to contain a large number, $v_\mathrm{c}\rho_\mathrm{c}(\boldsymbol{r}_n)$, of particles such that

$$1 \ll v_\mathrm{c}\rho_\mathrm{c}(\boldsymbol{r}_n) \ll N. \tag{3}$$

Thus, the coarse-grained density $\rho_c(\boldsymbol{r}_n)$ associated with the nth cell, whose centre is located at $\boldsymbol{r}_n$, is defined. Our program is then to coarse-grain (2) to derive the time-evolution equation for the coarse-grained density probability functional $P(\{\rho_c\}, t)$, which may take the form

$$\partial_t P(\{\rho_c\}, t) = \Omega_c P(\{\rho_c\}, t). \tag{4}$$

However, this program is not executed straightforwardly, because U_N in Ω_N contains interactions with inter-particle distance shorter than the coarse-graining cell size. This obstacle is bypassed in the following way. First, the functional $U\{\rho\}$ is expressed in terms of the original density variable ρ, reducing v_c to be infinitesimal. $U\{\rho\}$ thus obtained is bilinear in ρ. We assume then that the potential energy functional $U_c\{\rho_c\}$ is still expressible as a bilinear form in ρ_c after the coarse-graining but with the original potential density replaced by some effective potential energy density. At this stage the coarse-grained operator Ω_c in (4) is found to include the gradient of the chemical potential given by the functional derivative of the coarse-grained free-energy functional $H_c\{\rho_c\}$. The latter contains, in addition to the configurational entropy contribution associated with the arrangement of N particles into coarse-grained cells, the coarse-grained potential energy functional which is still fictitious in that the functional form of the effective potential energy density is not determined yet. If the coarse-grained free energy is expanded around the liquid state $\rho = \rho_0$ up to the second order in $\delta\rho(\boldsymbol{r})$, then the effective potential energy density in question is included in the second-order term. Noticing that the second-order term, when Fourier transformed followed by averaging over the liquid states with the density ρ_0, yields the static structure factor, which is then expressible in terms of the Fourier transform of the direct correlation function $C(r)$ [9], we can establish indirectly the relation between the effective potential energy density and the direct correlation function. In this way, the operator Ω_c in (4) is found to be given by

$$\Omega\{\rho\} = -\frac{D_0}{k_B T}\int \mathrm{d}\boldsymbol{r}\, \frac{\delta}{\delta\rho(\boldsymbol{r})}\nabla\cdot\rho(\boldsymbol{r})\left[k_B T\frac{\delta}{\delta\rho(\boldsymbol{r})} + \frac{\delta H\{\rho\}}{\delta\rho(\boldsymbol{r})}\right], \tag{5}$$

with the coarse-grained free energy [31]

$$H\{\rho\} = k_B T\int \mathrm{d}\boldsymbol{r}\,\rho(\boldsymbol{r})\left[\ln\frac{\rho(\boldsymbol{r})}{\rho_0} - 1\right] - \frac{1}{2}k_B T\iint \mathrm{d}\boldsymbol{r}\,\mathrm{d}\boldsymbol{r}'\, C(|\boldsymbol{r}-\boldsymbol{r}'|)\delta\rho(\boldsymbol{r})\delta\rho(\boldsymbol{r}'). \tag{6}$$

Note that hereafter we drop the subscript 'c' used to express explicitly coarse-grained quantities. In particular, $\rho(\boldsymbol{r})$ in (5) and (6) denotes the coarse-grained density, now regarded as a slowly varying continuous field, which should not be confused with the original density. The second term in the square brackets in (5) is the chemical potential which represents the thermodynamic driving force, whereas the first term carries the effect of thermal fluctuations. In this context, $\Omega\{\rho\}$ is said to be a stochastic time-evolution operator. The expression (6) is, except for a trivial difference, the same as that used to study freezing and glass transitions [31, 32].

We thus arrive at the closed coarse-grained description, given by (4)–(6), which expresses the time-evolution of the coarse-grained density field (see [3] for a full derivation).

We can also execute a coarse-graining procedure for a general one-component classical fluid. In this case, instead of executing the program faithfully, we take a shortcut by choosing as the starting description the nonlinear fluctuating hydrodynamics [26] mentioned in section 1.2, which already reaches the coarse-grained description (4) but the arguments contain the momentum field $\boldsymbol{g}(\boldsymbol{r})$ as well as the density field $\rho(\boldsymbol{r})$. As stated in section 1.2, our task is then to average out the field $\boldsymbol{g}(\boldsymbol{r})$ from the time-evolution equation. A systematic way for such a problem is to use the projection operator formalism [16]. However, the algebra is somewhat lengthy and hence only the final result is mentioned. As for further details of derivations, readers are referred to the original paper [3].

Surprisingly, quite the same time-evolution equation results as that found for a colloidal system with only a replacement of $D_0/(k_BT)$ by τ/m. Here τ is some time constant of the order of the local momentum relaxation, which should be regarded as the lower cutoff timescale of our coarse-grained description.

The following comment is in order at this point. MCT predicted that at long times the relaxation dynamics is independent of the microscopic dynamics adopted. This is evident also from our DDFT argument that the identical DDF equation results at longer times than the local momentum relaxation time. Indeed, we can derive [3] on the basis of (4) and (5) with further approximations of the same self-consistent equation which determines the long-time behaviour of the density correlator as that used in MCT [17, 33]. In order to corroborate the prediction computer simulations were carried out for a Lennard-Jones mixture [34] and a polydisperse mixture of colloidal particles [35] with both Newtonian and Brownian dynamics. It was found that the relaxation dynamics does, in fact, not depend on the microscopic dynamics in the α-relaxation regime [34].

2.2. Mapping onto lattice gas model

As is evident from the above argument, the DDF equation (4) with (5) is the most natural equation that embodies the idea that in sufficiently dense liquids the density is the only slow variable that describes local small scale motions. From this point of view, the computational works which simulate the Langevin equations containing the momentum and density variables are not satisfactory for studying late-stage dynamics in that a task of numerically solving the equations was realized only within the initial stage of freezing due to a numerical instability encountered at further supercooling [36].

In our DDFT approach, the momentum variable was analytically eliminated at the outset[3]. The resultant equation (4) is a closed stochastic equation, which includes the nonlinear feedback mechanism of MCT and at the same time permits us to study long-time behaviour even in the α-relaxation regime governed by the hopping process over the free-energy landscape described by the Ramakrishnan–Youssoff (RY) free-energy functional (6).

However, the DDF equation is strongly nonlinear and is still quite difficult to treat even numerically. We therefore present a substitute for equation (4) in the following heuristic argument.

Let us suppose a Kawasaki-type kinetic Ising model [37], which is in general, corresponding to (1), written by the following master equation for the probability distribution $P_0(\boldsymbol{n}, t)$:

$$\partial_t P_0(\boldsymbol{n}, t) = \mathcal{L}(\boldsymbol{n}) P_0(\boldsymbol{n}, t) \equiv \sum_{\boldsymbol{n}'} [w_0(\boldsymbol{n}|\boldsymbol{n}') P_0(\boldsymbol{n}', t) - w_0(\boldsymbol{n}'|\boldsymbol{n}) P_0(\boldsymbol{n}, t)], \tag{7}$$

where $\boldsymbol{n} = \{n_i\}$ denotes a set of occupation variables, $n_i = 0$ or 1 depending on whether the ith site is vacant or occupied, respectively, and $w_0(\boldsymbol{n}|\boldsymbol{n}')$ is the transition probability from $\boldsymbol{n}'$ to $\boldsymbol{n}$, to which the detailed balance condition is applied. Here the whole system has been divided into an assembly of primitive cells with the lattice constant h and spin exchanges are supposed to take place with equal probability between any pair of spins belonging to the nearest-neighbour coarse-graining cells, a coarse-graining cell consisting of many primitive cells. The energy entering the Ising model through $w_0(\boldsymbol{n}|\boldsymbol{n}')$ is given by

$$H_0(\boldsymbol{n}) = -\tfrac{1}{2} k_B T \sum_{i \neq j} C(|\boldsymbol{r}_i - \boldsymbol{r}_j|) n_i n_j, \tag{8}$$

[3] The conceptual difference between the Langevin dynamics method and our DDF formalism has been argued elsewhere [7] and is not repeated here.

where $C(r)$ is the direct correlation function of the reference liquid and $\boldsymbol{r}_i$ is the position vector of the ith site.

Here we set our coarse-graining length scale Λ, which should be appropriate for describing the phenomenon under consideration, by the following inequalities:

$$h \ll \Lambda \ll \sigma \sim l, \tag{9}$$

where σ and l are the range of $C(r)$ and the average inter-particle distance $\sim{\rho_0}^{-1/3}$, respectively. As for the concrete coarse-graining procedure of (7) with (8) we refer to [7]. The resultant time-evolution equation after taking the continuum limit becomes the DDF equation (4) with $H\{\rho\}$ taken to be the RY form (6). On the way to arrival at the DDF equation, we have assumed that ρ_0 is much smaller than ρ_m, ρ_m being the maximum density when all the lattice points in a coarse-graining cell are fully occupied, so that $\rho_\mathrm{m} - \rho(\boldsymbol{r})$ may be safely replaced by ρ_m. Thus, it can be said that the DDF equation (4) is (inversely) mapped onto the kinetic Ising model (7). We here call the latter the lattice version of DDFT.

In our lattice version of DDFT, the nonlinear feedback mechanism of density arrest central to MCT enters through the spin-exchange dynamics via the factor $\rho_0(\rho_\mathrm{m} - \rho_0) \simeq \rho_\mathrm{m}\rho_0$. Note that the factor is responsible for the excluded volume or steric hindrance property of spin exchange or 'particle' migration in the lattice gas language[4]. Thus, if the DDF equation (4) with (6) is going to exhibit glassy behaviour, this must be reflected in some way in the lattice DDF equation (7) with (8). Therefore, the studies of the latter as a substitute of the former might be quite rewarding, irrespective of the abovementioned approximation involved. What are presented below are the results obtained through a numerical investigation of the lattice DDFT, which is preceded by a brief account of the method of computation. Before closing this section we mention that an attempt was made to give a theoretical basis for the lattice DDFT by a sophisticated but formal argument [38].

3. Numerical computations

The whole system is a cube of side $L = \tilde{L}h$, which is divided into the computational lattice consisting of $\tilde{L}^3$ lattice points. As for the direct correlation function $C(r)$ in (8), which is the only input information for our lattice version DDFT besides ρ_0, Wertheim's solution [39] to the Percus–Yevick equation for HSS was employed. The hard sphere diameter σ involved in $C(r)$ is expressed in units of h as $\sigma = \tilde{\sigma}h$. We took $\tilde{L} = 15$ and $\tilde{\sigma} = 3.3$. See [4] for details which include the account of the choice of these values. We only mention that the present set-up, largely restricted by the computer resources available, does not seem to satisfy the coarse-graining condition (9). At this time the only thing we can do is to judge by the results obtained.

The successive configuration $\boldsymbol{n}(t)$ was generated using the ordinary Monte Carlo method, provided that the initial configuration is supplied, which was prepared by randomly occupying the lattice sites with the average density ρ_0 or hence the packing fraction $\eta = (1/6)\pi\rho_0\sigma^3$. That is, a Markov chain $\{|n(t)\rangle, |n(t+1)\rangle, \ldots, |n(t+m)\rangle\}$ was generated according to

$$|n(t+m)\rangle = \hat{\mathcal{L}}^m |n(t)\rangle, \tag{10}$$

where $\boldsymbol{n}$ is now represented by a state vector $|n(t)\rangle$ in the configuration space spanned by a set of $\tilde{L}^3$ basis vectors. $\hat{\mathcal{L}}$ in (10) represents the stochastic operator corresponding to $\mathcal{L}$ in (7), which was implemented by the heat bath method [40]. In order to avoid a trivial correlation between the consecutive $|n\rangle$'s thus generated, a number of $\tilde{L}^3$ configurations were generated

[4] The lattice gas particle does not directly correspond to a real constituent particle of a liquid and is distinguished from the latter by quotation marks. The difference between the two will be emphasized in section 3.2 below.

to increase the time in (10) by one, i.e. the time in the lattice version of DDFT is represented in units of Monte Carlo steps (MCS) per site.

3.1. Overall aspect

It is noted at first that, although the dependence of the *thermodynamic* state of an HSS on η has been established as shown in table 1, each value of those packing fractions does not necessarily yield the corresponding phase transition point in our system. This is due partially to the finiteness of our system but mainly due to an effect of discretization that cannot be easily estimated here. The latter effect originates from the discretization of an originally continuous free-energy functional, which is evaluated as the discrete Ising Hamiltonian (8) in our lattice DDFT. The situation quite resembles that which appeared in the Langevin dynamics method [36] in which RY free-energy [31] was discretized for computational purposes. Thus, the fact that values quite similar to those obtained for the freezing and crossover packing fractions in [36] (see below), which are different from those found in an actual system, does not seem accidental. We therefore have to begin with characterizing the state, or more specifically, *order*, of our system from the viewpoint of structural relaxation as a function of η.

In order to properly characterize the state of the system we define the following *reference state* $|\Psi_{\rm ref}^{(\alpha)}\rangle$ in terms of $|n\rangle$:

$$|\Psi_{\rm ref}^{(\alpha)}\rangle = \|\langle n\rangle_{t_2;t_1}^{(\alpha)}\|^{-1}|\langle n\rangle_{t_2;t_1}^{(\alpha)}\rangle, \tag{11}$$

where

$$|\langle n\rangle_{t_2;t_1}^{(\alpha)}\rangle \equiv \frac{1}{t_2}\int_{t_1}^{t_1+t_2} {\rm d}t'\,|n(t')\rangle. \tag{12}$$

This expresses the 'mobility' of $|n\rangle$ in the configuration space, which is strongly affected by barriers and valleys on the free-energy landscape that are developed with increasing supercooling. The origin t_1 should be taken to be sufficiently large to avoid possible initial transients, whereas the order of t_2 should be chosen to be that of the characteristic time under consideration. The states thus averaged over the timescale t_2 would depend on a particular basin, denoted by the superscript (α), to which the states belong. The property of the reference state is fully explained in [7].

The numerical factor in front of (11) accounts not only for the normalization of $|\Psi_{\rm ref}^{(\alpha)}\rangle$ but also gains meaning in assessing the amount of ergodicity of the system within the timescale of evaluation. Considering that we are treating the lattice gas model, some ideas from the spin glass theory may be taken over to prescribe the order of the system. Indeed, we can construct the Edwards–Anderson type order parameter [41] in terms of the norm $\|\langle n\rangle_{t_2;t_1}^{(\alpha)}\|$ as follows:

$$\Psi_{\rm EA}(t_2;t_1) = \frac{1}{\rho_0(1-\rho_0)}\frac{1}{\tilde{L}^3}\overline{\|\langle n\rangle_{t_2;t_1}^{(\alpha)}\|^2} - \frac{\rho_0}{1-\rho_0}, \tag{13}$$

where the overbar means an average over α. From preliminary calculations in which $t_1 = 100$ MCS was chosen but t_2 was extended up to 3×10^4 MCS, the liquid state could be divided into the following three regimes according to the qualitative behaviour of $\Psi_{\rm EA}$:

(i) regime $\eta < \eta_{\rm f} \simeq 0.43$, in which $\Psi_{\rm EA}$ decays quickly,
(ii) regime $\eta_{\rm f} < \eta < \eta_{\rm x} \simeq 0.49$, where $\Psi_{\rm EA}$ decays rather gradually; and
(iii) regime $\eta_{\rm x} < \eta$, where $\Psi_{\rm EA}$ never decays to zero.

Quite similar values for $\eta_{\rm x}$ as well as $\eta_{\rm f}$ were obtained by the Langevin dynamics method [36] in which a similar scale of discretization of the whole system was employed (see also [42]). We call these regimes the nominal liquid, the supercooled liquid and the deeply supercooled

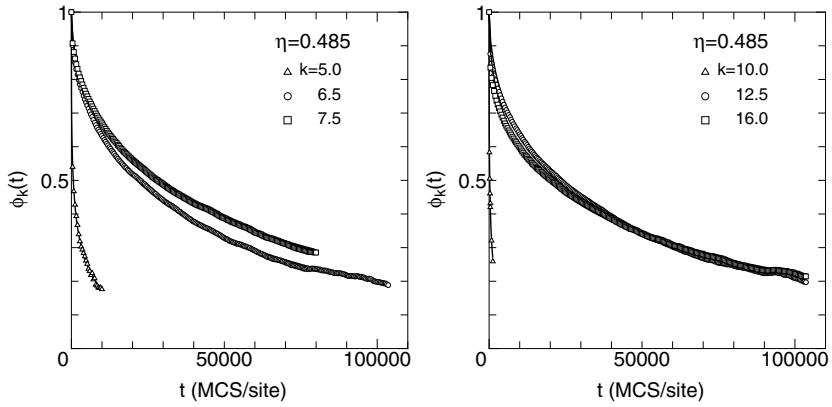

Figure 1. Time dependence of the density correlator ϕ_q at $\eta = 0.485$ in the supercooled liquid regime. Full curves (almost behind the symbols) represent fitted stretched exponential functions from which the exponent β_q and the relaxation time τ_q are determined (see table 2). The ϕ_q's with q around the primary peak position $k = q\sigma = 6.5$ of the structure factor are shown in the left panel, while the right panel shows this around the secondary peak position $k = 12.5$.

liquid or glassy regimes, respectively. It should be stressed that there is no strict criterion on the division of the regimes. In fact, no apparent discontinuities show up in the static properties such as the structure factor in passing from regime (i) into (ii). Note, however, the definitely qualitative difference in the relaxation below and above η_x, which was in fact identified as the crossover packing fraction (see below) formally denoted by η_c in the idealized MCT.

Before examining more closely the difference in relaxation behaviour associated with a change in the character of the free-energy landscape in those regimes, it is necessary to evaluate the timescale of the relaxation. To this end the normalized density correlator $\phi_q(t)$ was calculated for various packing fractions, from which the relaxation time τ_q as well as the exponent β_q were extracted by fitting the results to the stretched exponential function (see section 1.1). The values have already been tabulated in table 1 of [4][5]. However, we repeated the calculation to gain much better statistics by extending the time steps at least 100 times as large as those employed previously. This allows us to increase the time window of $\phi_q(t)$ by a factor of 2–3. Moreover, we added several points of η in the close vicinity of η_x at which these calculations were carried out. We show in figure 1 as an example the time variations of $\phi_q(t)$ for $\eta = 0.485$ in the supercooled liquid regime[6]. The left panel shows those with the wavenumber around the primary peak position $k = 6.5$ of the structure factor, while the right panel shows those around the secondary peak position $k = 12.5$. As to the typical structure factors for the three regimes, see figure 3 of [4]. The plateau, whose height gives the glass form factor as mentioned in section 1.1, is not recognizable from the figure, which might appear at first glance to be due to an inadequacy of our DDFT [43]. This point will be clarified in the next subsection. The full curves (though almost hidden by the symbols) represent fitted stretched exponential functions. The revised values obtained by the fit are tabulated in table 2. It will be identified later that these τ indeed yield the characteristic times of the late β- or α-relaxation regimes in the supercooled liquid state, which prompts us to fit the dependence of τ on η to a power-law form. This result is shown in figure 2, in which $D^{-1} \sim \tau$ at $k = 6.5$ is plotted

[5] Follow the link from http://wwwsoc.nii.ac.jp/jps/jpsj/index.html.

[6] We use the dimensionless wavenumber $k = q\sigma$ here.

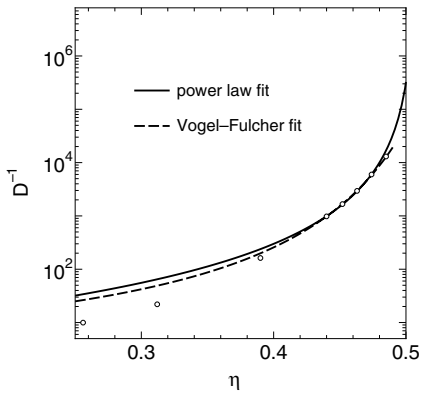

Figure 2. Dependence of the inverse diffusion constant, or the characteristic timescale of the α-relaxation, on the packing fraction.

Table 2. The characteristic time τ_q of the α-relaxation in units of MCS (left in each column) and the exponent β_q (right) obtained through a fit to a stretched exponential function as a function of packing fraction η and wavenumber given by $q\sigma$.

$q\sigma$	η	0.390		0.440		0.452		0.463		0.474		0.485	
5.0	25	0.81	130	0.60	200	0.45	340	0.48	810	0.54	1900	0.33	
6.5	83	0.86	910	0.67	1700	0.64	3900	0.63	9500	0.64	42000	0.55	
7.5	66	0.81	1100	0.65	2000	0.63	5000	0.63	12000	0.65	55000	0.53	
10.0	22	0.69	100	0.67	160	0.59	220	0.59	450	0.60	570	0.37	
12.5	44	0.72	770	0.59	1500	0.55	4300	0.54	11000	0.57	44000	0.54	
16.0	37	0.66	650	0.53	1300	0.45	3800	0.45	11000	0.45	42000	0.46	

against η by open circles. A full curve is a fit to $(\eta_c - \eta)^{-\gamma}$ with $\eta_c \simeq 0.50 \simeq \eta_x$ and[7] $\gamma \simeq 2.6$, which is not in conflict with the original MCT prediction. However, the same data can also be fitted to the Vogel–Fulcher (VF) law [8], giving $\eta_c \simeq 0.60$, which is close to the one obtained in [36]. In view of the fact that the VF law is discussed on a phenomenological basis, a slightly better fit to the VF law might have rather fortuitous significance and we do not look into this point any further.

Having thus evaluated the typical relaxation timescale in the three regimes of the liquid state, we return to the argument of the manner of structural relaxation in these regimes. We fix $t_2 \sim \tau \sim 10^3$ MCS, the typical relaxation time in the supercooled liquid regime, to tentatively define $|\Psi_{\rm ref}^{(\alpha)}\rangle$ for each[8] η. We then define the state $|\phi_t^{(\alpha)}\rangle$ in a similar manner by

$$|\phi_t^{(\alpha)}\rangle \equiv \| \langle n \rangle_{\tau;t}^{(\alpha)} \|^{-1} |\langle n \rangle_{\tau;t}^{(\alpha)}\rangle, \tag{14}$$

which enables us to assess a departure of $|\phi_t^{(\alpha)}\rangle$ at time t from the reference state $|\Psi_{\rm ref}^{(\alpha)}\rangle$ by the projection

$$q(t) = \langle \phi_t^{(\alpha)} | \Psi_{\rm ref}^{(\alpha)} \rangle. \tag{15}$$

Time evolutions of $q(t)$ thus defined are depicted in figure 3 for representative packing fractions in the three liquid regimes. In the nominal liquid regime ($\eta = 0.312$) q takes an almost constant value of unity (shown by a full curve). This is easily understandable from our

[7] Since the change at around η_x seems to be sluggish, it need not strictly distinguish $\eta_x \simeq 0.49$ from 0.50.

[8] t_1 is taken to be much longer.

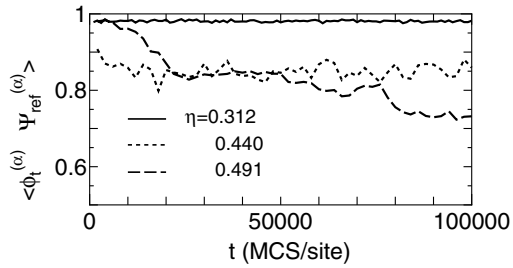

Figure 3. Time evolution of $q(t)$ at $\eta = 0.312$ (full curve), $\eta = 0.440$ (short broken curve) and $\eta = 0.491$ (long broken curve). At $\eta = 0.491$, which is just above the crossover packing fraction η_x, the system, which once was trapped in one of the glassy minima, starts to escape towards the state with lower free energy, while below η_x the system continues to stay in the liquid minimum though the amplitude of density fluctuations becomes larger as the packing fraction increases. Reproduced from [5].

expectation that in this regime there is a unique global minimum in the liquid free energy in which the system relaxes in a much shorter time than τ so that $|\phi_t^{(\alpha)}\rangle$ is independent of t and is essentially the same as $|\Psi_{\rm ref}^{(\alpha)}\rangle$. In this sense there is a unique α in this regime. As the packing fraction increases beyond η_f into the supercooled liquid regime, the amplitude of oscillation in q becomes larger with a slight loss of overlap but the centre of oscillation remains unchanged (short broken curve). This suggests that the liquid free-energy minimum, which is still a single minimum, becomes shallow[9].

It is a challenge to go beyond η_x where the original MCT is no longer accessible. A long broken curve shows a behaviour of q at η slightly above[10] η_x. After an initial jump q becomes almost flat, which is followed by a next jump. One can easily infer that the system gets trapped in one of the glassy minima from which it eventually relaxes toward a lower free-energy state via thermally activated hopping transitions over free-energy barriers. This peculiar behaviour of q thus provides strong evidence for the hopping process. The timescale associated with the hopping process, which is estimated from the duration between successive jumps, seems to be at least one order of magnitude longer than τ, an upper bound of the timescale over which the original MCT can cope with.

In order to examine in more detail the change in the landscape with a change in η, which is speculated from the qualitative change in the behaviour of q, we introduce the order parameter $q_{\alpha\beta}$ defined by

$$q_{\alpha\beta} \equiv \langle \Psi_{\rm ref}^{(\alpha)} | \Psi_{\rm ref}^{(\beta)} \rangle \qquad (\alpha \neq \beta). \tag{16}$$

This is, so to speak, the replica order parameter in the spin glass language [44], which measures the amount of overlap between different reference states. To obtain $q_{\alpha\beta}$ 20 realizations with different initial configurations were generated to calculate $|\Psi_{\rm ref}^{(\alpha)}\rangle$ at each packing fraction. Consult the original paper [5] for computational details.

The distributions of the values of $q_{\alpha\beta}$ are shown in figure 4. In the nominal liquid regime, the distributions are sharply peaked at around unity, implying the uniqueness of the liquid free-energy minimum. However, this 'replica symmetry' breaks down with increasing packing fraction beyond η_f, reflecting the multi-minima aspect of the free-energy landscape. At the same time the average of the distribution tends to a smaller value, which means that the average 'distance' between the reference states becomes larger.

[9] The decrease in overlap is due to slightly insufficient equilibration upon evaluation of the reference state.
[10] It is more appropriate to state that η is in the crossover region.

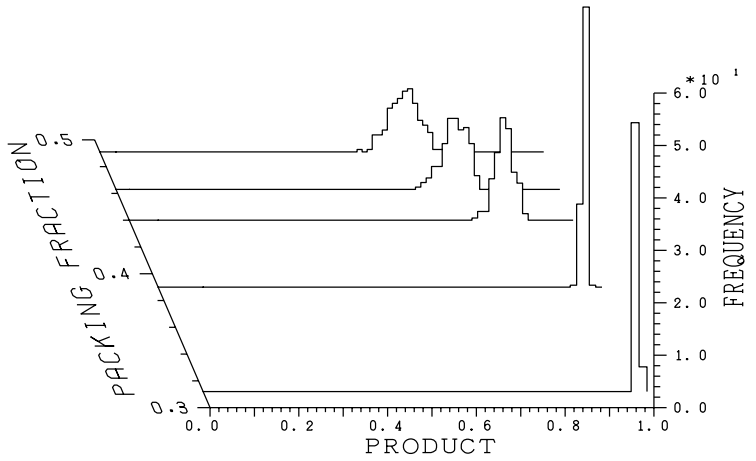

Figure 4. Distributions of the order parameter $q_{\alpha\beta}$ obtained from 20 realizations of the reference states $\{|\Psi_{\rm ref}^{(\alpha)}\rangle\}$ with different initial configurations at each packing fraction. These are, from the lower packing fraction side, at $\eta = 0.312$, 0.390, 0.440, 0.463 and 0.491. Reproduced from [5].

We have thus succeeded in discussing the glassy dynamics of liquid in connection with the free-energy landscape, utilizing the spin glass analogy in a novel way. This could be done because our lattice version of DDFT is constructed on the kinetic lattice gas model.

3.2. Advantage of coarse-grained description

As described in section 2.2 our lattice version of DDFT provides a coarse-grained description up to the length scale $\sim\sigma$. This brings about a great advantage over the other approaches reviewed in the introduction, as we shall see below. In connection with this point an explanation for the 'particle' mentioned in section 2.2 should be given here in some detail.

From the fact that $\boldsymbol{n}(t)$ of the lattice DDFT is only related to the local particle density $\rho(\boldsymbol{r}, t) = \sum_i \delta(\boldsymbol{r} - \boldsymbol{r}_i)$ in the continuum by the relation $\langle n_i \rangle_\tau = \langle \rho(\boldsymbol{r}, t) \rangle_\tau$, the average being taken over the typical relaxation times, together with the coarse-graining of (9) applied to the kinetic lattice gas model, it is evident that the 'particle' of the lattice gas model does not directly represent a liquid particle. They coincide at the dilute gas limit where the mean-free path is the only length scale of the system. Moreover, identity of a liquid particle is lost during the coarse-graining. This means that the lattice DDFT cannot treat the motion of a tagged particle. To be more specific, the van Hove function, which is given in the lattice DDFT by $G(\boldsymbol{r}, t) = \tilde{L}^{-3} \sum_{ij} \langle \delta n_i(t) \delta n_j(0) \rangle \delta_{\boldsymbol{r}, \boldsymbol{r}_i - \boldsymbol{r}_j}$, where $\delta n_i = n_i - \rho_0$, is meaningful in the lattice DDFT but its self and distinct parts are not. The same argument can be used for the intermediate scattering function, the spatial Fourier transform of $G(\boldsymbol{r}, t)$, whose time variations were already shown as the density correlator in the previous subsection.

However, although a 'particle' is not a particle by itself, the motion of particles ought to be reflected through the Kawasaki exchange of 'particles' [45]. Depicted in figure 5 are time variations of the mean squared displacement (MSD) of a tagged 'particle' under various packing fractions. Delineated by broken curves are those in the nominal liquid regime, whereas full curves are in the supercooled liquid regime. Note that the behaviour of MSD in figure 5 bears hardly any similarity with the ordinary MSD behaviour such as the one reported for HSS in figure 4 of [14], the reason being given in the following. When compared with the corresponding result obtained through the microscopic dynamics method such as MD

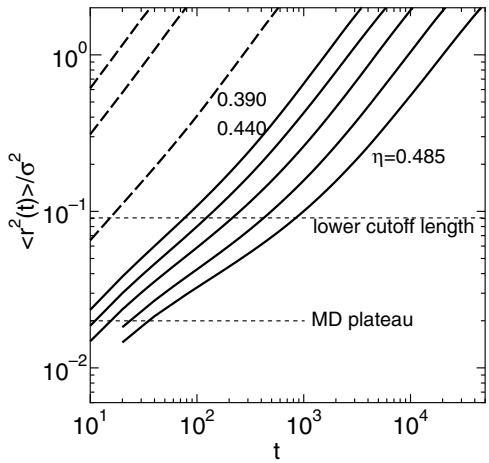

Figure 5. MSD versus time in units of MCS of a 'particle' for various packing fractions; from the top $\eta = 0.256$, 0.312, 0.390, 0.440, 0.452, 0.463, 0.474 and 0.485.

simulations, naturally no regime of ballistic motion is present. It is also seen that in the supercooled regime the plateau in MSD associated with the cage effect, which *should* appear at around $\langle r^2(t)\rangle/\sigma^2 \simeq 2 \times 10^{-2}$ [46], is obscure and the motion of 'particles' gradually goes over into a diffusive behaviour. This is quite reasonable, however, because the height of the plateau is *below* the present lower-cutoff length, which is given in terms of MSD as $\langle r^2\rangle/\sigma^2 \simeq 10^{-1}$. At around this height slight inflection is recognized in the curves of MSD. One can also extract from this figure the lower-cutoff time $t_{\rm lc}$ for each η, which is given by $\langle r^2(t_{\rm lc})\rangle/\sigma^2 \simeq 10^{-1}$. The dynamical processes with timescales less than $t_{\rm lc}$ should be regarded as fictitious.

The moments $\langle r^{2n}(t)\rangle$ $(n = 1, 2, \ldots)$ of a tagged 'particle' can be calculated in a similar way, from which the non-Gaussian parameter $\alpha_n(t) = \langle r^{2n}(t)\rangle/(C_n\langle r^2(t)\rangle^n) - 1$ with $C_n = (2n+1)!!/3^n$ [47] is obtainable. The non-Gaussian parameter α_2 thus obtained is presented in figure 6. Those parts in the fictitious time region are omitted. It is said that the non-Gaussian nature of 'particle' motion is pronounced at around the time regimes where the plateau in MSD would appear, the time regimes where the cage effect would be pronounced in real particle motions.

Shown in figure 7 are ϕ_q for various packing fractions plotted versus $t/\tau_q(\eta)$ (see table 2 for τ_q) for $k \equiv q\sigma = 7.5$ corresponding to the wavenumber in the immediate vicinity of the primary peak in the structure factor. We can now address the problem of the absence of the MCT plateau associated with the early β-relaxation (the location being designated in the figure as $\phi_k(\infty)$), which *is* in the fictitious time domain. However, the two-stage relaxation, i.e. the β-relaxation followed by the α-relaxation, observed in the dynamic light scattering for colloidal systems mentioned in section 1.1 *should* be reproducible by a stochastic model like DDFT, which is in no way the same as a totally microscopic description containing inertia effects. We shall come back to this point in the next section.

It is rather important, however, to appreciate that the density correlators obtained through the lattice DDFT thus skip over the stage leading to the plateau, the way of approaching the plateau being known to be strongly affected by the microscopic dynamics employed [34, 35], and immediately show the asymptotic scaling behaviour in the supercooled liquid regime. This is nothing but the feature that is brought about by the effectiveness of the coarse-grained

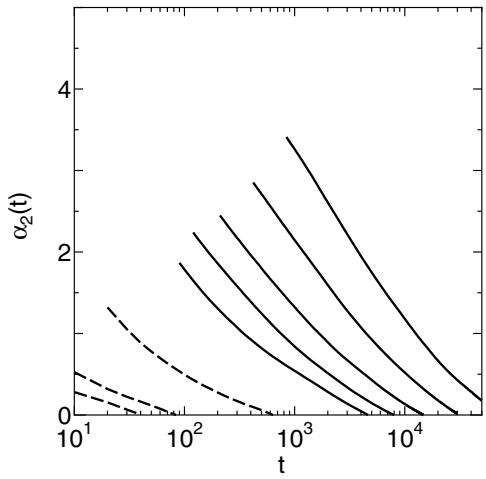

Figure 6. The non-Gaussian parameter $\alpha_2 = 3\langle r^4\rangle/(5\langle r^2\rangle^2) - 1$ versus time in units of MCS at, from left to right, $\eta = 0.256$, 0.312, 0.390, 0.440, 0.452, 0.463, 0.474 and 0.485. The parts with t below the lower-cutoff time are not shown.

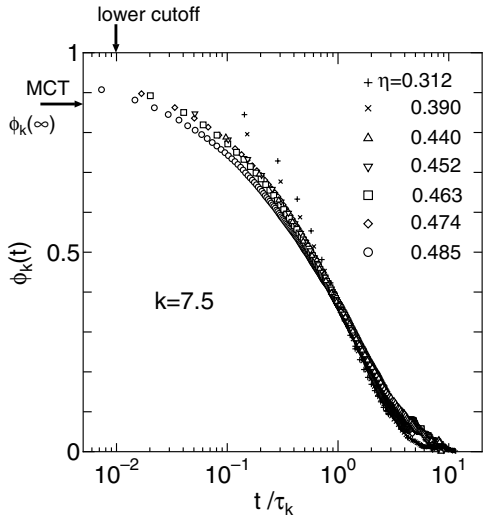

Figure 7. The normalized density correlator ϕ_q with $k = q\sigma = 7.5$ for various packing fractions are plotted against t/τ_q, τ_q being the α-relaxation timescale (see table 2). The states with $\eta = 0.312$ and 0.390 are in the nominal liquid regime, whereas the others are in the supercooled liquid regime.

description in treating the slow dynamics at the cost of the information regarding the plateau. The master curve formed by the plots for η in the supercooled liquid regime (note that $\eta = 0.312$ and 0.390 are in the ordinary liquid regime) shows the α-relaxation of the density correlator. This is why we fitted the density correlator to the stretched exponential form in the previous subsection. Figure 7 is the lattice DDFT demonstration of the time–temperature superposition principle predicted by the original MCT. In this connection we have no desire to compete with MCT in the region where the idealized MCT is valid (the regime in which thermally activated processes play no role). Our aim is to provide a way to naturally extend the results of MCT to the region with non-negligible thermally activated processes.

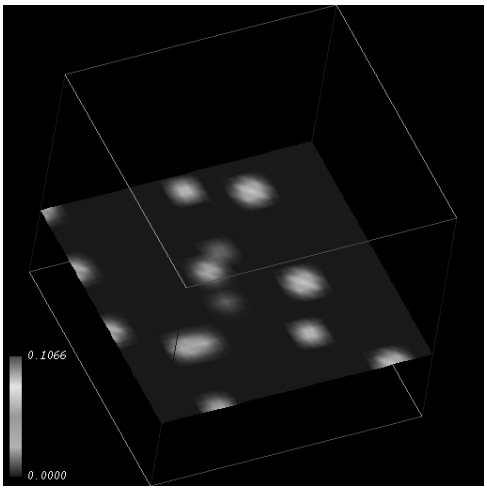

Figure 8. Sectional view of the coarse-grained density profile at $\eta = 0.491$.

The other advantage of our coarse-grained description is that the density profile evolving in time is directly obtainable. The density profile, when averaged over a suitable time duration, varies from wave-like diffusive to particle-like strongly localized pattern with increasing packing fraction, as shown in figure 1 of [4]. In this way, we could visualize the coarse-grained density profile to show that actual jumping of particles takes place during the hopping transition over the glassy free-energy landscape (figure 3) in the deeply supercooled liquid regime (see figure 3 of [5]). The 'wave–particle duality' of the density profile may also be a useful feature in discussing a possible escape route of a structurally arrested particle in a deeply supercooled liquid. Such a particle image was indeed detected which deformed as if it was divided into two or more when passing through a narrow canal during an activation process. An example seen in $\eta = 0.491$ is shown in figure 8, in which such elongated images are noticeable. Such an activation process consists of frequent exchange between 'particles' and 'holes', whose frequency and spatial distribution may have a close connection with the kinetic heterogeneity associated with bond breakage processes [48].

4. Discussion and future perspective

Historically, essentially the same kinetic equation as the DDF equation (4) with (5) has been already put forth before the MCT breakthrough but in different contexts [49], which were not studied extensively. Recently, Munakata [50] has developed the DDF formalism. However, caution should be used in a blind application of the mode-coupling approximation to the purely dissipative kernel [38, 51] (see also [52] for the irreducible memory function method).

Yet another DDFT has been proposed recently by Marconi and Tarazona [53]. In their formalism, on the way to a conversion of the Langevin equation for particle motion to the time-evolution equation of the density field, the free-energy functional of the inhomogeneous field naturally appears. They assumed that the evolution of the system can be represented by an infinite sequence of *equilibrium* states $\rho(\boldsymbol{r}, t)$ that make the *grand potential functional* $F_{\mathrm{canon}}\{\rho\}$ a minimum. The resultant DDF equation is a deterministic one that describes the evolution of the averaged density field driven by the gradient of the chemical potential. However, it is clear from its construction that their DDF equation cannot deal with

the first passage problem such as barrier crossing discussed in the last subsection, since the grand potential becomes unstable there.

Of particular importance is that they pointed out that the free-energy functional which enters other existing DDFT, including ours, is the microcanonical one. It is thus appropriate to comment on two types of free-energy density functionals in general [43]. One is that introduced in the equilibrium theory of liquid [54]. Here we imagine a liquid in a *stable* equilibrium state under an external field acting on the density, which is a function of $\boldsymbol{r}$. Thus the Helmholtz free-energy depends on the external field. If we apply a Legendre transform, we get a so-called canonical free-energy density functional $F_{\rm canon}$ which is always stable by construction. We note that the unique correspondence between external field and density profile is proven [55]. Due to this stability property this functional cannot be used to discuss metastability or, especially, instability because the Hessian matrix $\delta^2 F_{\rm canon}/(\delta\rho(\boldsymbol{r})\delta\rho(\boldsymbol{r}'))$ is always positive semi-definite. On the other hand, in application to dynamics another type of free-energy density functional is often introduced by specifying the density profile $\rho(\boldsymbol{r})$ precisely, which may be called the microcanonical density functional $F_{\rm micro}$. There is no guarantee that the Hessian matrix for $F_{\rm micro}$ has to be positive definite, and can be used to study metastable and unstable states. However, virtually no serious study exists for $F_{\rm micro}$. Various approximate forms proposed for $F_{\rm canon}$, such as the RY density functional [31], is smuggled in to replace[11] $F_{\rm micro}$. However, the difference between the two density functionals becomes small if the density fluctuations are kept small by choosing large enough coarse-graining cells. For the reference fluid of our lattice version of DDFT, this is the case since the size of a coarse-graining cell can be taken to be between h and l (see (9)). Therefore, the problem mentioned here disappears for the reference fluid.

It is appropriate at this point to make a comment on the criticism raised by Marconi and Tarazona [53]. They claimed that, although our coarse-graining procedure is physically motivated, it cannot be rendered explicit. This does not hold for the lattice version of DDFT at least, as is evident from the arguments presented in section 3.2. Recall the absence of the MCT plateau in the decay of the density correlator, which is a consequence of our choice of the coarse-graining scale specified by the inequalities (9). In the lattice DDFT the choice of this scale *is* at our disposal. If a larger σ than the current value is adopted, then we may look into the time regime of the MCT plateau. We hope to prove this proposition in the near future.

Although the lattice version of DDFT proved to be fruitful as seen in section 3, we must repeat that the mapping onto the kinetic lattice gas model is merely an approximate one (see section 2.2). The degree of the approximation becomes worse as supercooling proceeds, i.e. with increasing packing fraction. Since the approximation is based on the physically plausible argument and does not proceed in a systematic way, we can no longer assess how much poorer the approximation will become. This point should be clarified before applying the lattice DDFT to a more complex system or to new kinds of systems not yet treated by other means.

Conceptual difficulty is still inherent in our DDFT, as pointed out by one of the authors [43]. This is in regard to the elimination of variables without clear-cut separation of timescales. In our current DDFT the momentum field was projected out, based on an intuitive argument, although the projection itself was carried out analytically (see section 2.1). This is only

[11] It is a curious fact that this RY density functional does not always describe stable states. This is due to the fact that the RY form is obtained by expansion in powers of the local density fluctuation around its average value in the stable uniform liquid state. However, equilibrium free-energy can have singularities, e.g. essential singularity at the first-order phase transition as shown by Fisher and Andreev [56], which is washed away by expansion. The RY free energy thus can be analytically continued into inside the coexistence region just as for the original van der Waals theory. This makes the RY form qualify as a free energy that can be used to deal with metastability and instability.

adequate in the high-temperature region where taking the high-friction limit in the Kramers rate theory [57] is justifiable. Therefore in high-packing fraction regimes not only the lattice version of DDFT but also the original DDFT may be confronted with a difficulty attributed to the physical situation which is not taken into consideration in the formalism. Our DDFT is still an infant in this sense. We must continue to pay much effort in looking for a way to surmount or bypass this point. Yet, enormous slowing-down of the density variable in the low temperature and/or high density regime tends to favour clear-cut separation of time scales.

As to this problem one of the authors has recently suggested [43] the use of action variables as a substitute for local density, which might give a gleam of hope. The action variables appear in the instantaneous normal-mode approach [58] to the barrier crossing problem. The phase–space variables in the configuration space are transformed into normal-mode variables with real and imaginary eigenfrequencies corresponding to local stable and unstable points. These normal-mode variables are characterized by two widely separated timescales with which to divide them unambiguously into slow action and fast angle variables. A way of constructing a new DDFT, in which the latter variables are eliminated by coarse-graining procedure, has been proposed [43].

Finally we close this paper by making a comment on the way that DDFT makes sense in its own right to truly overcome MCT in examining the glass transition phenomena. As is clear from the argument thus far, the usefulness of DDFT will hinge on the accountability of the experimental results on the glass side beyond the crossover point. We believe that the DDF formalism will provide a promising way to attack this problem, although some inherent difficulties mentioned above in our current version of DDFT must be overcome in a satisfactory manner.

Acknowledgments

KF wishes to thank Japan Society for the Promotion of Science, Nippon Sheet Glass Foundation for Materials Science and Engineering, and Elektel Ozaki Foundation for financial support. Support for KK by the Cooperative Research under the Japan–US and Japan–Germany Cooperative Science Programs sponsored by Japan Society for the Promotion of Science is also gratefully acknowledged. All the numerical computations were carried out using the supercomputers installed at the Institute for Solid State Physics, the University of Tokyo and Yukawa Institute for Theoretical Physics, Kyoto University.

Appendix. Comment on section 6 of [59]

Since DDFT was discussed in some detail in [59], it is appropriate here to mention a delicate point associated with DDFT, which has not been touched upon so far, in the form of a comment here. We find it better to replace the rhs of equation (6.5) of that reference by

$$P_{\mathrm{e}}(\{\rho\},\{\boldsymbol{j}\}) = \tilde{P}_{\mathrm{e}}^{j}(\{\rho\},\{\boldsymbol{j}\})\tilde{P}_{\mathrm{e}}^{\rho}(\{\rho\})$$

where, apart from trivial constant normalization factors,

$$\tilde{P}_{\mathrm{e}}^{j}(\{\rho\},\{\boldsymbol{j}\}) \equiv \exp\left[-\int \mathrm{d}\boldsymbol{r}\,\frac{\boldsymbol{j}(\boldsymbol{r})^2}{2mk_{\mathrm{B}}T\rho(\boldsymbol{r})} - \frac{1}{2\Delta V}\int \mathrm{d}\boldsymbol{r}\,\ln\rho(\boldsymbol{r})\right]$$

and

$$\tilde{P}_{\mathrm{e}}^{\rho}(\{\rho\}) \equiv \exp(-\beta H_{\mathrm{corr}})$$

with

$$H_{\rm corr}(\{\rho\}) \equiv H(\{\rho\}) - \frac{k_{\rm B}T}{2\Delta V}\int {\rm d}\boldsymbol{r}\ \ln\rho(\boldsymbol{r}).$$

Here ΔV is the coarse-graining volume. Each factor on the rhs is normalized in the sense that $\int {\rm d}\{\boldsymbol{j}\}\ \tilde{P}_{\rm e}^{j}(\{\rho\},\{\boldsymbol{j}\})$ and $\int {\rm d}\{\rho\}\ \tilde{P}_{\rm e}^{\rho}(\{\rho\})$ are both constants independent of $\{\boldsymbol{j}\}$ and $\{\rho\}$.

It should be noted that $H_{\rm corr}$ is the correct free-energy functional that appears in the equilibrium probability distribution for $\{\rho\}$ which *differs* from H that appears in the Fokker–Planck operator (5).

If we regard $\boldsymbol{j}$ as a vector with three independent components, the factor 3 is required in front of the logarithmic terms in the above. However, in the MCT context, only the longitudinal component of the momentum density field comes in, and hence the factor 3 is absent. In other contexts this factor is required.

References

[1] Bengtzelius U, Götze W and Sjölander A 1984 *J. Phys. C: Solid State Phys.* **17** 5915
Leutheusser E 1984 *Phys. Rev.* A **29** 2765
[2] Stillinger F H 1995 *Science* **267** 1935
Ediger M D, Angell C A and Nagel S R 1996 *J. Phys. Chem.* **100** 13200
[3] Kawasaki K 1994 *Physica* A **208** 35
Kawasaki K 1998 *Progress in Statistical Physics* ed W Sungi *et al* (Singapore: World Scientific) p 28
Kawasaki K 1998 *J. Stat. Phys.* **93** 527
[4] Fuchizaki K and Kawasaki K 1998 *J. Phys. Soc. Japan* **67** 1505
[5] Fuchizaki K and Kawasaki K 1998 *J. Phys. Soc. Japan* **67** 2158
[6] Kawasaki K and Fuchizaki K 1998 *J. Non-Cryst. Solids* **235–237** 57
[7] Fuchizaki K and Kawasaki K 1999 *Physica* A **266** 400
[8] Angell C A 1988 *J. Phys. Chem. Solids* **49** 863
Kudlik A, Benkhof S, Blochowicz T, Tschirwitz C and Rössler E 1999 *J. Mol. Struct.* **479** 201
[9] Hansen J-P and McDonald I R 1986 *Theory of Simple Liquids* (London: Academic)
[10] Pusey P N and van Megen W 1986 *Nature* **320** 340
Paulin S E and Ackerson B J 1990 *Phys. Rev. Lett.* **64** 2663
[11] van Megen W and Underwood S M 1993 *Phys. Rev. Lett.* **70** 2766
[12] van Megen W and Underwood S M 1993 *Phys. Rev.* E **47** 248
[13] van Megen W and Underwood S M 1994 *Phys. Rev.* E **49** 4206
[14] van Megen W, Mortensen T C, Williams S R and Müller J 1998 *Phys. Rev.* E **58** 6073
[15] Tokuyama M and Oppenhiem I 1994 *Phys. Rev.* E **50** R16
[16] Zwanzig R 1961 *Lectures in Theoretical Physics* vol 3, ed W E Britton, B W Downs and J Downs (New York: Wiley)
Mori H 1965 *Prog. Theor. Phys.* **33** 423
[17] Götze W 1991 *Liquids, Freezing and the Glass Transition (Les Houches Session LI, 1989)* ed J-P Hansen, D Levesque and J Zinn-Justin (Amsterdam: North-Holland) p 287
[18] Fuchs M 1994 *J. Non-Cryst. Solids* **172–174** 241
[19] Götze W and Sjögren L 1992 *Rep. Prog. Phys.* **55** 241
Götze W 1999 *J. Phys.: Condens. Matter* **11** A1
[20] Kob W 1997 *Experimental and Theoretical Approaches to Supercooled Liquids: Advances and Novel Applications* ed J Fourkas, D Kivelson, U Mohanty and K Nelson (Washington, DC: American Chemical Society) p 28
Kob W 1999 *J. Phys.: Condens. Matter* **11** R85
[21] Barrat J L, Götze W and Latz A 1989 *J. Phys.: Condens. Matter* **1** 7163
[22] Götze W and Sjögren L 1988 *J. Phys. C: Solid State Phys.* **21** 3407
[23] Sjögren L 1990 *Z. Phys.* B **79** 5
Fuchs M, Götze W, Hilderbrand S and Latz A 1992 *J. Phys.: Condens. Matter* **4** 7709
[24] Cummins H Z, Du W M, Fuchs M, Götze W, Hilderbrand S, Latz A, Li G and Tao N J 1993 *Phys. Rev.* E **47** 4223
Cummins H Z, Li G, Hwang Y H, Shen G Q, Du W M, Hernandez J and Tao N J 1997 *Z. Phys.* B **103** 501

[25] Kawasaki K 1995 *Transp. Theory Stat. Phys.* **24** 755
[26] Das S P and Mazenko G F 1986 *Phys. Rev.* A **34** 2265
[27] de Schepper I M and Cohen E G D 1982 *J. Stat. Phys.* **27** 223
[28] Cohen E G D and de Schepper I M 1992 *Recent Progess in Many-Body Theories* ed T L Ainsworth *et al* (New York: Plenum)
[29] Hohenberg P C and Halperin B I 1977 *Rev. Mod. Phys.* **49** 435
Bray A 1994 *Adv. Phys.* **43** 357
[30] Zwanzig R 1969 *Adv. Chem. Phys.* **15** 325
[31] Ramakrishnan T V and Yussouff M 1979 *Phys. Rev.* B **19** 2775
[32] Singh Y, Stoessel J P and Wolynes P G 1985 *Phys. Rev. Lett.* **54** 1059
Dasgupta C and Ramaswamy S 1992 *Physica* A **186** 314
[33] Ackerson B J 1978 *J. Chem. Phys.* **69** 684
[34] Gleim T, Kob W and Binder K 1998 *Phys. Rev. Lett.* **81** 4404
[35] Löwen H, Hansen J-P and Roux J-N 1991 *Phys. Rev.* A **44** 1169
[36] Lust L M, Valls O T and Dasgupta C 1993 *Phys. Rev.* E **48** 1787
Valls O T and Mazenko G F 1991 *Phys. Rev.* B **44** 2596
Dasgupta C and Valls O T 1996 *Phys. Rev.* E **53** 2603
[37] Kawasaki K 1966 *Phys. Rev.* **145** 224
[38] Kawasaki K 1998 *Bussei Kenkyu* **69** 810
[39] Wertheim M S 1963 *Phys. Rev. Lett.* **10** 321
[40] Binder K 1979 *Monte Carlo Methods in Statistical Physics* ed K Binder (Berlin: Springer) p 1
[41] Edwards S F and Anderson P W 1975 *J. Phys. F: Met. Phys.* **5** 965
[42] Dasgupta C 1992 *Europhys. Lett.* **20** 131
[43] Kawasaki K 2000 *J. Phys.: Condens. Matter* **12** 6343
[44] Dotsenko V 2001 *Introduction to Replica Theory of Disordered Statistical Systems* (Cambridge: Cambridge University Press)
[45] Fuchizaki K 2000 *J. Physique* IV **10** Pr7-37
[46] Kob W, Nauroth M and Andersen H C 1997 *Prog. Theor. Phys. Suppl.* **126** 21
[47] Rahman A 1964 *Phys. Rev.* **136** A405
[48] Yamamoto R and Onuki A 1997 *J. Phys. Soc. Japan* **66** 2545
[49] Munakata T 1977 *J. Phys. Soc. Japan* **43** 1723
Bagchi B 1987 *Physica* A **145** 273
[50] Munakata T 1996 *Aust. J. Phys.* **49** 25
[51] Jäckle J 1994 *Disorder Effects on Relaxation Processes* ed R Richert and A Blumen (Berlin: Springer) p 233
[52] Kawasaki K 1995 *Physica* A **215** 61
[53] Marconi U M B and Tarazona P 1999 *J. Chem. Phys.* **110** 8032
Marconi U M B and Tarazona P 2000 *J. Phys.: Condens. Matter* **12** A413
[54] Evans R 1979 *Adv. Phys.* **28** 143
[55] Chayes J T and Chayes L 1984 *J. Stat. Phys.* **36** 471
[56] Fisher M E 1967 *Physics* **3** 225
Andreev A F 1964 *Sov. Phys.–JETP* **18** 1415
[57] Kramers H A 1940 *Physica* **7** 284
[58] Keyes T 1997 *J. Phys. Chem.* A **101** 2921
[59] Kawasaki K 2000 *Recent Res. Devel. Stat. Phys.* **1** 41